An Extended Doherty Amplifier With High Efficiency Over a Wide Power Range

Masaya Iwamoto, *Student Member, IEEE*, Aracely Williams, Pin-Fan Chen, *Member, IEEE*, Andre G. Metzger, *Student Member, IEEE*, Lawrence E. Larson, *Fellow, IEEE*, and Peter M. Asbeck, *Fellow, IEEE*

***Abstract*—An extension of the Doherty amplifier, which maintains high efficiency over a wide range of output power (>6 dB), is presented in this paper. This extended Doherty amplifier is demonstrated experimentally with InGaP/GaAs heterojunction bipolar transistors at 950 MHz. Power-added efficiency (PAE) of 46% is measured at P_{1dB} of 27.5 dBm and 45% is measured at 9 dB backed off from P_{1dB}. Additionally, PAE of at least 39% is maintained for over an output power range of 12 dB backed off from P_{1dB}. This is an improvement over the classical Doherty amplifier, where high efficiency is typically obtained up to 5–6 dB backed off from P_{1dB}. Compared to a single transistor class-B amplifier with similar gain and P_{1dB}, the extended Doherty amplifier has PAE 2.6× higher at 10 dB back off and 3× higher at 20 dB back off from P_{1dB}. Under different bias and output matching conditions, the amplifier was also evaluated with CDMA signals. At the highest measured power of 25 dBm, the extended Doherty amplifier achieves a PAE of 45% with an adjacent channel power ratio of −42 dBc. Generalized design equations are also derived and the consequences of finite device output impedance on amplifier gain and linearity are explored.**

***Index Terms*—CDMA, heterojunction bipolar transistors, power-added efficiency, RF power amplifier.**

I. Introduction

POWER control of RF transmitters is a key requirement in modern digital telephony. For example, in the case of CDMA, power control is implemented in both the base station and handset transmitters [1]. Power control in the base-station transmitter mitigates the "corner" problem in which mobile units near the edges of a cell require more power due to transmission losses and adjacent cell interference. It also minimizes interference to the mobile units in the adjacent cells. On the mobile unit side, it is very important for handsets to transmit power at variable levels so that signals received by the base station are similar in strength for all users to maximize system capacity. Owing to such an aggressive system requirement, it is common for power amplifiers in *mobile* transmitters to operate at output power levels of 10–40-dB backoff from peak power. Unfortunately, a significant consequence of this requirement is that the power amplifier operates mostly within regions of low efficiency. Since the power amplifier uses a large portion of the battery power in handsets, it is desirable for amplifiers in these applications to have higher efficiencies at backoff power to extend battery life. A promising efficiency boosting technique to achieve this result is the Doherty amplifier (Fig. 1), in which power from a main amplifier and an auxiliary amplifier are combined with appropriate phasing [2]–[9]. This paper explores an extension to the classical Doherty amplifier to enhance efficiency at lower output power.

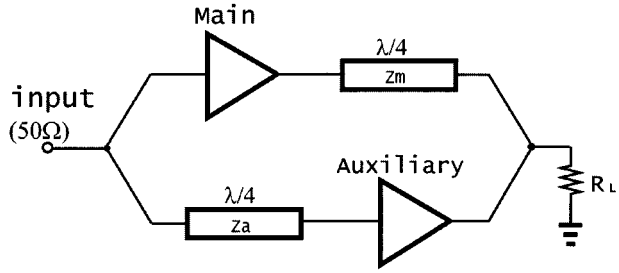

Fig. 1. Doherty amplifier topology.

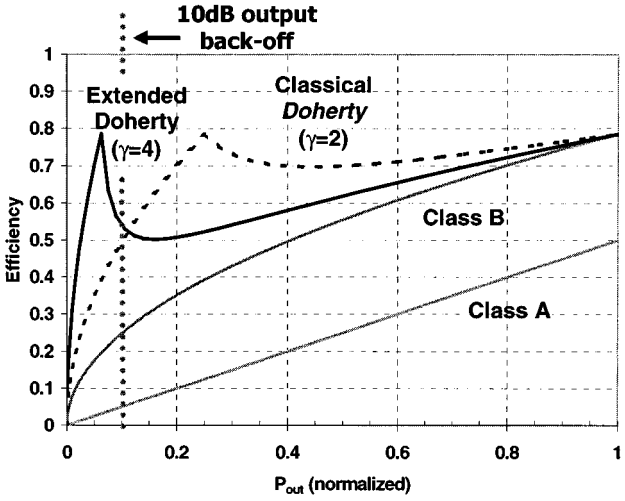

Fig. 2. Comparison of calculated efficiency characteristics.

Fig. 2 shows a comparison of efficiency characteristics of various power amplifiers. In the classical Doherty amplifier operation, high efficiencies are obtained over a nominal 6 dB of output power range. Raab analytically showed the possibility of extending the peak efficiency region over a wider range of output power [3]. In this paper, we experimentally demonstrate

Manuscript received March 30, 2001; revised August 23, 2001. This work was supported by the University of California at San Diego Center for Wireless Communications and by the Army Research Office Multidisciplinary University Research Initiative.

M. Iwamoto, A. Williams, L. E. Larson, and P. M. Asbeck are with the Department of Electrical and Computer Engineering, University of California at San Diego, La Jolla, CA 92092 USA.

P.-F. Chen was with Global Communications Semiconductors, Torrance, CA 90501 USA. He is now with Agilent Technologies, Santa Clara, CA 95050 USA.

A. G. Metzger is with the Department of Electrical and Computer Engineering, University of California at San Diego, La Jolla, CA 92092 USA and is also with Mindspeed Technologies, Newbury Park, CA 91320 USA.

Publisher Item Identifier S 0018-9480(01)10440-0.

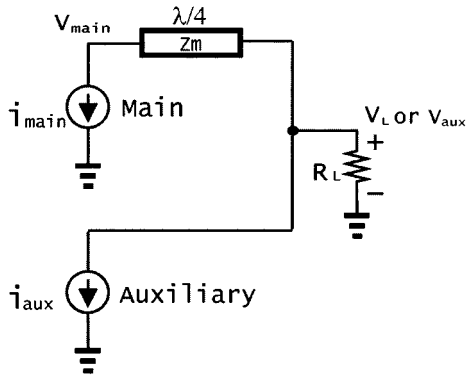

Fig. 3. Simplified output network used for analysis.

an extended Doherty amplifier with high efficiency over a wider range of output power compared to a classical Doherty design. The output power range between the two peaks in power-added efficiency (PAE) (as seen in Fig. 2) of 9 dB is achieved with a careful design of the input and output matching networks. In Section II, the basic principle of operation and a derivation of the design equations are presented. The analysis assumes the output of the transistors to be ideal current sources where the impedance is infinite. Therefore, in Section III, a similar, but a more realistic analysis is done considering the finite impedances at the output of the transistors. Detailed design and implementation issues of the amplifier are discussed in Section IV and experimental results are presented in Section V.

II. Principle of Operation and Analysis

The Doherty amplifier consists of main and auxiliary amplifiers with their outputs connected by a quarter-wave transmission line (Z_m). There is a quarter-wave transmission line (Z_a) at the input of the auxiliary amplifier to compensate for the equivalent delay at the output. The main amplifier is typically biased class B and the auxiliary amplifier is typically biased class C, so that the auxiliary amplifier turns on at the power when the main amplifier reaches saturation. The current contribution from the auxiliary amplifier reduces the effective impedance seen at the main amplifier's output. This "load–pulling" effect allows the main amplifier to deliver more current to the load while it remains saturated. Since an amplifier in saturation typically operates very efficiently, the total efficiency of the system remains high in this high-power range until the auxiliary amplifier saturates.

Fig. 3 illustrates a simple model for the Doherty amplifier, in which the transistor outputs are modeled as current sources controlled by their input voltages. i_{main} is assumed to be linearly proportional to the input signal voltage. Using superposition, voltages at the output of the main amplifier and the load are calculated to be

$$V_{\text{main}} = \frac{Z_m^2}{R_L} i_{\text{main}} - jZ_m i_{\text{aux}} \tag{1}$$

$$V_L = -jZ_m i_{\text{main}}. \tag{2}$$

In this ideal analysis, where the current sources have inherently infinite impedance, the load voltage is only a function of i_{main} since i_{aux} experiences a short circuit looking into the quarter-wave transformer at the output branch. However, since V_{main} is a function of i_{aux} in (1), i_{aux} influences the impedance looking out of the main amplifier and thereby controls the saturation behavior of the main amplifier.

If i_{critical} is defined as the value of i_{main} when the main amplifier reaches saturation, then i_{aux} can be chosen in relation to i_{main} as

$$i_{\text{aux}} = \begin{cases} 0, & i_{\text{main}} < i_{\text{critical}} \\ -j\gamma\left(i_{\text{main}} - i_{\text{critical}}\right), & i_{\text{main}} \geq i_{\text{critical}} \end{cases} \tag{3}$$

where γ is a design parameter that determines the value of i_{critical} in relation to $i_{\text{max\_main}}$, the maximum value of i_{main} as follows:

$$i_{\text{critical}} = \frac{1}{\gamma} i_{\text{max\_main}}. \tag{4}$$

Some important points should be mentioned regarding (3). First, i_{aux} is proportional to $-j$ times i_{main} since i_{aux} has to lag i_{main} by 90° for proper Doherty operation. Also, the parameter γ plays an important role in determining the relationship between i_{aux} and i_{main}. The relationship in (3) implies that the gain ratio between the main and auxiliary amplifiers should be adjusted depending upon the value of γ.

With $\gamma = 2$, the classical operation of the Doherty amplifier is obtained where i_{critical} is one-half that of $i_{\text{max\_main}}$. Since the region of high efficiency is given by the expression $20\log_{10}(\gamma)$ in decibels, $\gamma = 2$ results in a peak efficiency starting from about 6 dB backed off from peak power. It is apparent that the main amplifier can be made to saturate at a lower fraction of $i_{\text{max\_main}}$ by choosing a higher value of γ. Here, we define an "extended Doherty amplifier" to be a design with $\gamma > 2$.

To continue the analysis, the value of Z_m is obtained by inserting i_{aux} (3) into the expression for V_{main} (1), and solving for Z_{m} that makes V_{main} a constant, or saturated, value

$$Z_m = \gamma R_L \tag{5}$$

where V_{main} is

$$V_{\text{main}} = \begin{cases} \dfrac{Z_m^2}{R_L} i_{\text{main}}, & \text{i}_{\text{main}} < i_{\text{critical}} \\ \dfrac{Z_m^2}{R_L} i_{\text{critical}}, & i_{\text{main}} \geq i_{\text{critical}} \end{cases} \tag{6}$$

V_{main} becomes a constant value when $i_{\text{main}} \geq i_{\text{critical}}$, which is consistent with the Doherty operation.

Fig. 4(a) and (b) graphically summarizes (1)–(6). Fig. 4(a) shows V_{main} and V_L (or V_{aux}) as a function of i_{main}. V_{main} increases proportionally to i_{main} with a slope of $\gamma^2 R_L$ and reaches a constant saturated value $V_{\text{max\_main}}$ at i_{critical}. Fig. 4(b) shows i_{main} and i_{aux} plotted against i_{main}. This graph is useful in determining the maximum currents of the two amplifiers. Since γ is the slope of i_{aux} with respect to i_{main}, the value of maximum current of i_{aux}, $i_{\text{max\_aux}}$, in relationship to $i_{\text{max\_main}}$ can be determined as

$$i_{\text{max\_aux}} = (\gamma - 1) i_{\text{max\_main}}. \tag{7}$$

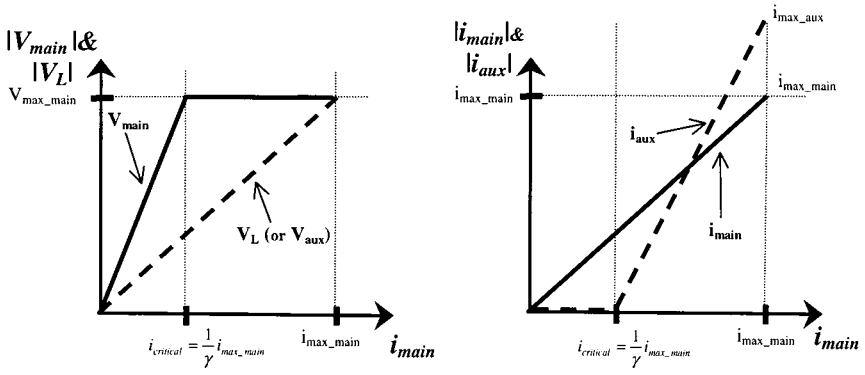

Fig. 4. (a) Voltage and (b) current characteristics as a function of $i_{\rm main}$.

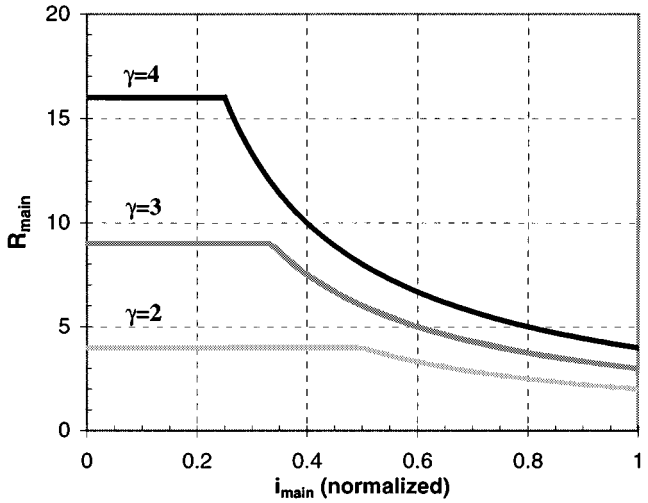

Fig. 5. $R_{\rm main}$ as a function of $i_{\rm main}$ with various γ values.

If the same peak current density is desired for both devices, then the size of the auxiliary amplifier should be $\gamma - 1$ times that of the main amplifier.

Using expressions for γ, $V_{\rm main}$ and V_L, the effective load seen by the main and auxiliary amplifiers can be analytically obtained for low drive power ($i_{\rm main} < i_{\rm critical}$) and peak power conditions ($i_{\rm main} = i_{\rm max\_main}$) as follows:

$$R_{\rm main} = \gamma^2 R_L, \qquad i_{\rm main} < i_{\rm critical} \tag{8}$$

$$\left.\begin{aligned} R_{\rm main} &= \gamma R_L \\ R_{\rm aux} &= \frac{\gamma}{\gamma - 1} R_L \end{aligned}\right\}, \qquad i_{\rm main} = i_{\rm max\_main}. \tag{9}$$

Fig. 5 shows a graphical representation of (8) and (9) for $R_{\rm main}$. R_L and $i_{\rm max\_main}$ are set to unity for this representative plot. It can be seen that with larger values of γ, $R_{\rm main}$ is also larger. In Section III, the consequences of increasing γ on the characteristics of the Doherty amplifier are explored.

III. Influence of Finite Device Output Impedance

From the analysis in Section II, it would seem possible to choose γ to be an arbitrary large value to boost efficiency at much lower output power. However, the analysis was rather simplified since an ideal output current source with infinite impedance was assumed. With a large value of γ, (8) shows that the effective load presented to the main amplifier can be potentially comparable to the device output impedance at low power drive. In this scenario, it would be relevant to examine the influence of the finite device output impedance. A more realistic analysis of the Doherty amplifier is examined in this section where finite impedances at the output of the main and auxiliary amplifiers are considered.

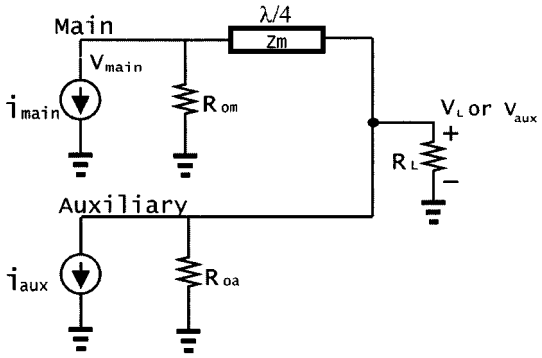

Fig. 6. Doherty output network with finite device output impedance.

The Doherty output network with finite device output impedance is shown in Fig. 6. The circuit is identical to the one in Fig. 3, except for the shunt resistors R_{om} and R_{oa} representing the output impedances of the main and auxiliary amplifiers, respectively. Again, using superposition and defining R_{Le} as the parallel combination of R_L and $R_{oa}(R_{Le} = R_L \| R_{oa})$, the voltages at the main amplifier output and the load are found to be

$$V_{\rm main} = \frac{R_{om} Z_m}{R_{Le} R_{om} + Z_m^2}\left(Z_m i_{\rm main} - j i_{\rm aux} R_{Le}\right) \tag{10}$$

$$V_L = \frac{R_{Le} Z_m}{Z_m^2 + R_{om} R_{Le}}\left(-j i_{\rm main} R_{om} + i_{\rm aux} Z_m\right). \tag{11}$$

The expression for V_L is significantly different from the infinite output impedance case [see (2)] in that it is a function of both $i_{\rm main}$ and $i_{\rm aux}$. Using the same definition of $i_{\rm aux}$ in (3), V_L now becomes a nonlinear function of $i_{\rm main}$ (which is proportional to the input signal voltage). This implies that there will be AM–AM distortion as a result of the finite output impedance of the devices. Also, the presence of finite output impedance

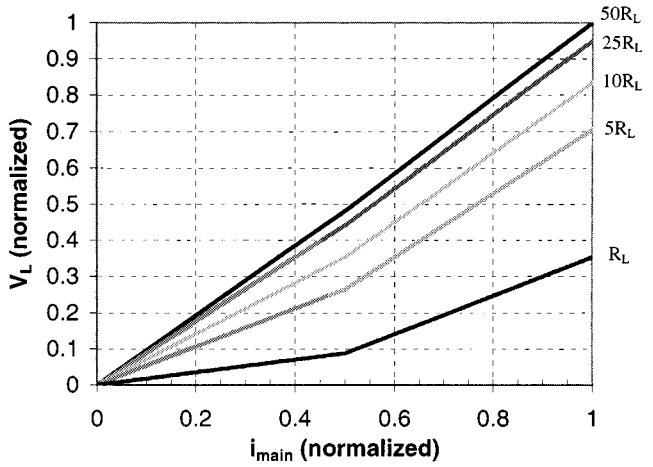

(a)

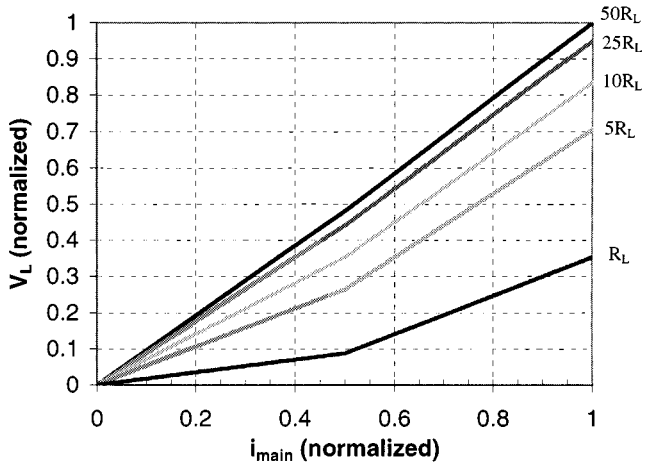

(b)

Fig. 7. Plot of V_L versus i_{main} for: (a) $\gamma = 2$ and (b) $\gamma = 4$. Shown on the right-hand side are the values of R_{om} and R_{oa} with respect to R_L.

in (11) reduces the value of V_L, which results in a decrease in gain. Plots of V_L versus i_{main} are shown in Fig. 7(a) and (b) with various values of R_{om} and R_{oa} for $\gamma = 2$ and $\gamma = 4$, respectively. It is evident that the decrease in gain and presence of AM–AM distortion are discernible when R_{om} and R_{oa} become comparable to R_L. However, when R_{oa} and R_{ob} become larger, (10) and (11) approach (1) and (2), respectively. These trends are also observable in Fig. 7, where for high values of R_{om} and R_{oa}, V_L resembles a linear relationship with i_{main}, as in (2). In any case, the analysis stresses the importance of large device output impedance for Doherty amplifiers with large values of γ.

To finish off the analysis, Z_m can be calculated by substituting i_{aux} in (11) with (3) and solving for Z_m that makes V_{main} a constant value

$$Z_m = \gamma R_{Le} \tag{12}$$

and

$$V_{\text{main}} = \begin{cases} \dfrac{R_{oa} Z_m^2}{R_{Le} R_{oa} + Z_m^2}\, i_{\text{main}}, & i_{\text{main}} < i_{\text{critical}} \\ \dfrac{R_{oa} Z_m^2}{R_{Le} R_{oa} + Z_m^2}\, i_{\text{critical}}, & i_{\text{main}} \geq i_{\text{critical}}. \end{cases} \tag{13}$$

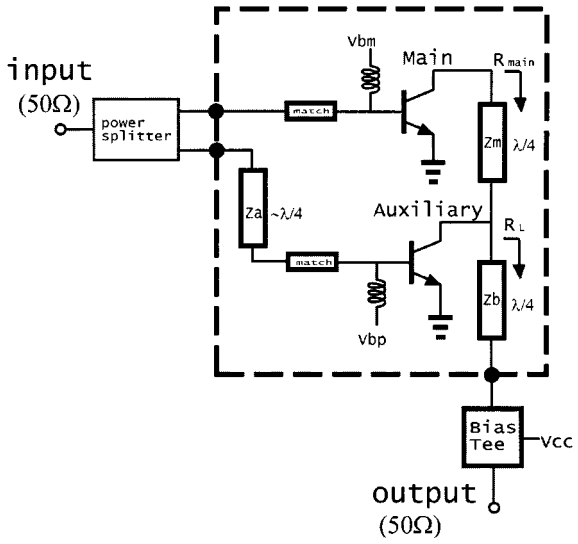

Fig. 8. Implementation of the extended Doherty amplifier.

It can be seen that V_{main} is still consistent with the infinite device impedance case where it is a linear function of i_{main} for $i_{\text{main}} < i_{\text{critical}}$ and a constant value for $i_{\text{main}} \geq i_{\text{critical}}$. However, the value of V_{main} decreases as R_{om} and R_{oa} become comparable to R_L.

IV. Design and Implementation Issues

A 950-MHz 0.5-W extended Doherty amplifier with $\gamma = 4$ was designed with InGaP/GaAs heterojunction bipolar transistors (HBTs) using microstrip on a printed circuit board with 60-mil-thick FR-4 dielectric ($\varepsilon_r \sim 4.3$, $\tan\delta = 0.025$). The HBTs were wire bonded on to Tech-Ceram microwave packages. HBTs were chosen for their high current handling capabilities, as well as high output impedances to prevent the effects described in the previous section. A simplified circuit schematic is shown in Fig. 8.

From the analysis in Section II, the parameter γ influences several important aspects of the Doherty amplifier design. First, it determines the transition point where the auxiliary amplifier turns on according to (4). With $\gamma = 4$, the region of high efficiency should ideally start approximately at 12-dB backoff from peak output power. Secondly, γ determines the impedance characteristics of the output network. According to (8) and (9), $\gamma = 4$ results in the effective load seen by the main amplifier at low drive power to be $16R_L$ and at peak power to be $4R_L$.R_L is chosen to be 4.5 Ω in accordance with load line considerations for the transistor characteristics of the auxiliary amplifier. The impedance transformation from the output (50 Ω) to $R_L = 4.5\ \Omega$ is done using a quarter-wave microstrip line ($Z_b = 15\ \Omega$) and the quarter-wave transformation from R_L to the output of the main amplifier ($R_{\text{main}} = 72\ \Omega$) is also done using microstrip ($Z_m = 18\ \Omega$). By using microstrip for the output impedance transformations, biasing the collectors of the two transistors (with $V_{\text{CC}} = 4$ V) is facilitated with external bias tees. Thirdly, γ determines the scaling ratio between the main and auxiliary amplifiers if similar maximum current densities are desired. With $\gamma = 4$, (7) states that the ideal scaling ratio between the auxiliary and main amplifiers to maintain the same

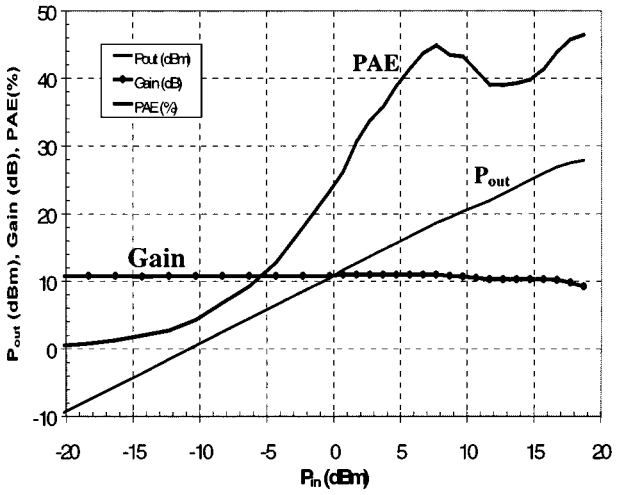

Fig. 9. Output power, gain, and PAE as a function of input power.

current densities at maximum power should be 3 : 1. However, due to availability issues of the power HBT devices, a scaling ratio of 4 : 1 was chosen, with total emitter areas of 3360 and 840 μm^2 for the auxiliary and main amplifiers, respectively. Finally, γ influences the rate at which the effective load at the main amplifier ($R_{\rm main}$) is pulled down when the auxiliary amplifier is turned on. Therefore, γ determines the saturation characteristics of the main amplifier, which, in turn, affects gain flatness, efficiency, and linearity. Equation (3) implies that the gain ratio between the two amplifiers is γ and, furthermore, the gain of the auxiliary amplifier should be greater than the gain of the main amplifier. This gain ratio can be accommodated by adjusting the sizes of the two devices, the input match of each amplifier, and the power-splitting ratio at the input. Since the auxiliary amplifier is biased in class C, it is typically difficult to match the gain of this amplifier to be greater than the main amplifier unless the overall gain is sacrificed. Therefore, a practical method to achieve the proper gain ratio is to divide the power at the input in an unequal fashion. It was determined in simulations that using a 1 : 2 power divider [10] between the inputs of the main and auxiliary amplifiers resulted in proper Doherty operation for $\gamma = 4$. By having twice the power delivered to the auxiliary amplifier than the main amplifier, gain flatness and good efficiency were achieved in the output power range when the auxiliary amplifier was on. Additionally, it was found that adjusting the delay in the auxiliary amplifier input path (Z_a) was critical for proper Doherty operation. This delay was adjusted so that the output of the auxiliary amplifier lagged the output of the main amplifier by 90°.

V. Measurement Results

A. One-Tone Test

Single-tone measurements were made on the extended Doherty amplifier at 950 MHz. Fig. 9 shows a power sweep with measured output power, PAE, and gain as a function of input power. The characteristic behavior of the Doherty amplifier is apparent from the fact that the PAE reaches an initial peak and remains high until peak power is reached. This initial peak in PAE at 45% (which is approximately when the main amplifier saturates and the auxiliary amplifier turns on) occurs at an output power of 18.5 dBm. $P_{\rm 1dB}$ is at 27.5 dBm with a PAE of 46%. The output power range between these two critical points is 9 dB. This result is an improvement over the classical Doherty amplifier, where this high efficiency region is typically 5–6 dB backoff from $P_{\rm 1dB}$. Additionally, PAE of at least 39% is maintained over an output power range of 12 dB from $P_{\rm 1dB}$.

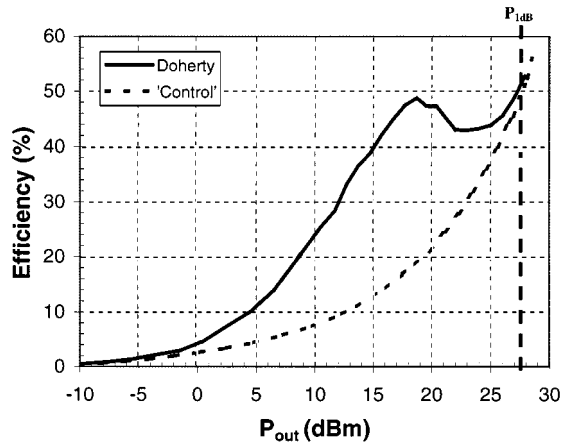

(a)

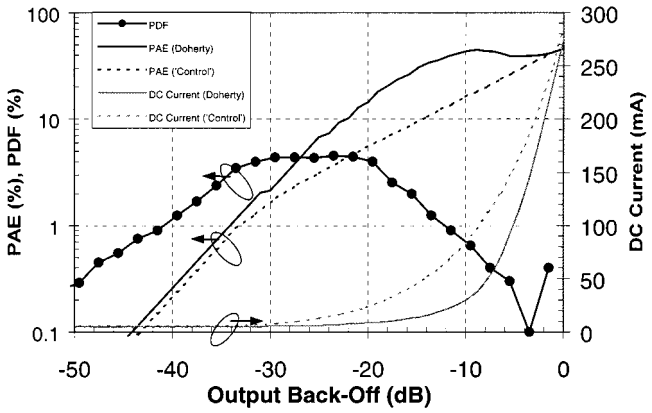

(b)

Fig. 10. Performance comparison of the extended Doherty and "control" amplifiers. (a) Total collector efficiency versus output power. (b) PAE and dc current versus output backoff from $P_{\rm 1dB}$ and PDF of a representative CDMA mobile transmitter output power.

A single transistor "control" amplifier (equivalent to a class-B amplifier) with similar gain, $P_{\rm 1dB}$, output bias voltage, and quiescent current was designed using the same HBT as the auxiliary amplifier for comparison purposes. Fig. 10(a) shows a comparison of collector efficiencies of the extended Doherty and "control" amplifiers as functions of output backoff. It is clearly visible that the efficiency of the extended Doherty is considerably higher at backoff power. PAE and dc currents for both amplifiers are plotted versus output backoff from $P_{\rm 1dB}$ in Fig. 10(b). Also shown is a probability density function (or power usage profile) of a representative mobile transmitter. The significant advantage of the extended Doherty amplifier is evident when its efficiency characteristics and the probability of transmission are considered together. For example, PAE of 43.5% is measured at 10-dB backoff, and PAE of 15% is measured at 20-dB backoff from $P_{\rm 1dB}$, where for the "control" amplifier, PAE is only 16.5% and 5%, respectively.

For systems with varying probability of transmission, it is relevant to define an overall system efficiency. Using the definition from Hanington *et al.* [11], system efficiency is given by

$$\eta_{\text{ave}} = \frac{\langle P_{\text{out}} \rangle}{\langle P_{\text{in}} \rangle} \tag{14}$$

where $\langle P_{\text{out}} \rangle$ and $\langle P_{\text{in}} \rangle$ are average weighted input and output powers given by

$$\langle P_{\text{out}} \rangle = \int_0^{+\infty} p\left(P_{\text{out}}\right) P_{\text{out}}\, dP_{\text{out}} \tag{15}$$

$$\langle P_{\text{in}} \rangle = \int_0^{+\infty} p\left(P_{\text{out}}\right) P_{\text{in}}\left(P_{\text{out}}\right)\, dP_{\text{out}}. \tag{16}$$

Using the input and output characteristics of the extended Doherty and "control" amplifiers, as well as the probability distribution function (PDF) for IS-95 signals in an urban environment [information all contained in Fig. 10(b)], the average system efficiencies are calculated to be

$$\eta_{\text{ave}} = 24.3\% \quad \text{(Extended Doherty)}$$
$$\eta_{\text{ave}} = 14.7\% \quad \text{("Control").}$$

As expected, the average efficiency for the extended Doherty amplifier is considerably higher than the "control" amplifier.

The peak PAE level is limited by several factors. It is anticipated that further improvements could be obtained by using a printed-circuit-board material with lower dielectric loss, by reducing the transistor packaging parasitics, and by implementing optimized harmonic terminations.

B. CDMA Measurements

For the previous measurements, the amplifier was designed and biased for the proper Doherty efficiency performance as a function of output backoff, and linearity was not considered. To evaluate the performance of the amplifier for wireless communication applications with CDMA signals, slight modifications were made in order to simultaneously optimize efficiency and linearity. Second and third harmonic traps were placed at the outputs of the main and auxiliary amplifiers, respectively, as shown in Fig. 11. With this harmonic termination strategy, the main amplifier output experiences a short at the second harmonic and an open at the third harmonic. This is because the $\lambda/4$ line Z_m is equivalent to a $\lambda/2$ line at the second harmonic and a $3\lambda/4$ line (which has an impedance transformation equivalent to a $\lambda/4$ line) at the third harmonic. By doing so, the main amplifier resembles a class-F amplifier, which should have high efficiency when it is operating at large RF swings. To avoid excessive large-signal nonlinearities such as AM–AM and AM–PM distortion, the main amplifier is kept out of deep saturation by optimizing the turn-on behavior of the auxiliary amplifier. This is done by controlling the bias and drive of the auxiliary amplifier. Since the main amplifier is kept well out of deep saturation, the efficiency will be lower than that of the typical Doherty curve, as shown in Fig. 9, but will remain significantly higher than for a single transistor class-AB amplifier. The bias arrangements were also modified. It was found that the linearity

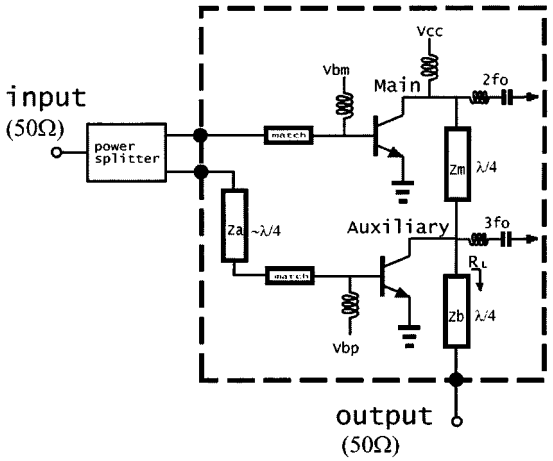

Fig. 11. Circuit of the extended Doherty amplifier optimized for linearity.

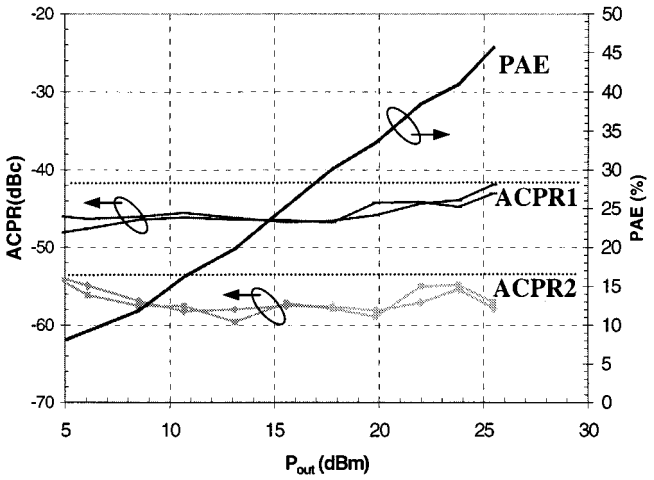

Fig. 12. Measured ACPR and PAE versus output power.

of the Doherty amplifier measured with broad-band input signals (such as CDMA signals) is particularly sensitive to the bias circuit impedance at the baseband (over the input signal bandwidth). This occurs since the main and auxiliary amplifiers stay in the large-signal swing condition over a wide power range, and their supply currents vary significantly with variations of signal envelope.

Fig. 12 shows the measured results of adjacent channel power ratio (ACPR) and PAE plotted versus output power for CDMA signals in the amplifier of Fig. 11. The ACPR1 limit of -42 dBc and the ACPR2 limit of -54 dBc (corresponding to IS-98 specifications) are met up to the highest measured output power of 25 dBm. The high values of ACPR2 at low power are attributed to the noise floor of the measurement system. Although the PAE is lower than that shown in Fig. 9 (as is typical for CDMA rather than single-tone inputs), PAE of 45% is measured at the highest measured power. At 10-dB backoff, PAE is still high at 23%, while for typical class-AB amplifiers, the PAE at this backoff power is about a factor of four lower than at the peak efficiency. Overall power efficiency was calculated using (14) with the PDF shown in Fig. 10(b) for CDMA signals. The resulting efficiency was calculated to be 17.5%, which is still higher than the single-transistor class-B transistor measured under single-tone

excitation, as described above. These linearity and efficiency results are promising for handset transmitter applications. Further efficiency improvements can also be anticipated with optimized design.

VI. Conclusions

A 0.5-W extended Doherty amplifier with high efficiency over a wide range of output power was demonstrated with InGaP/GaAs HBTs. At $P_{1\mathrm{dB}}$ of 27.5 dBm, PAE of 46% was measured and at 9-dB backoff from $P_{1\mathrm{dB}}$, PAE of 45% was measured. Also, PAE of at least 39% was maintained over a range of 12-dB backoff from $P_{1\mathrm{dB}}$. Under CDMA excitation and different bias and loading conditions, PAE of 45% was measured at an output power of 25 dBm with and ACPR level of -42 dBc. With the need of higher efficiencies at low power in wireless communications, the extended Doherty amplifier may potentially play an important role in such applications.

Acknowledgment

The authors would like to thank Global Communication Semiconductors, Torrance, CA, for donating the power HBTs. The authors also appreciate discussions with H. Kobayashi, Fuji Electric, Nagano, Japan, and the University of California at San Diego (UCSD), C. Wang, UCSD, J. Salonen, UCSD, J. Hinrichs, UCSD, and M. Wetzel, UCSD, K. Gard, Qualcomm Inc., San Diego, CA, and helpful advice related to printed circuit boards from C. Bourde, Agilent Technologies, Santa Rosa, CA, H. Barnes, Agilent Technologies, Santa Rosa, CA, B. Thompson, Agilent Technologies, Santa Rosa, CA, and X. Qin, Agilent Technologies, Santa Rosa, CA.

References

[1] S. Soliman, C. Wheatley, and R. Padovani, "CDMA reverse link open power control," in *GLOBECOM'92*, pp. 69–73.
[2] W. H. Doherty, "A new high efficiency power amplifier for modulated waves," *Proc. IRE*, vol. 24, pp. 1163–1182, Sept. 1936.
[3] F. H. Raab, "Efficiency of Doherty RF power-amplifier systems," *IEEE Trans. Broadcast.*, vol. BC-33, pp. 77–83, Sept. 1987.
[4] R. J. McMorrow, D. M. Upton, and P. R. Maloney, "The microwave Doherty amplifier," in *IEEE MTT-S Int. Microwave Symp. Dig.*, 1994, pp. 1653–1656.
[5] C. F. Campbell, "A full integrated Ku-band Doherty amplifier MMIC," *IEEE Microwave Guided Wave Lett.*, pp. 114–116, Sept. 1999.
[6] K. W. Kobayashi, A. K. Oki, A. Gutierrez-Aitken, P. Chin, L. Yang, E. Kaneshiro, P. C. Grossman, K. Sato, T. R. Block, H. C. Yen, and D. C. Streit, "An 18–21 GHz InP DHBT linear microwave Doherty amplifier," in *RFIC Symp. Dig.*, 2000, pp. 179–182.
[7] C. P. McCarroll, G. D. Alley, S. Yates, and R. Matreci, "A 20 GHz Doherty power amplifier MMIC with high efficiency and low distortion designed for broad band digital communication systems," in *IEEE MTT-S Int. Microwave Symp. Dig.*, 2000, pp. 537–540.
[8] S. C. Cripps, *RF Power Amplifiers for Wireless Communications*. Norwood, MA: Artech House, 1999, pp. 225–239.
[9] P. B. Kenington, *High-Linearity RF Amplifier Design*. Norwood, MA: Artech House, 2000, pp. 494–506.
[10] H.-R. Ahn and I. Wolff, "General design equations of three-port unequal power-dividers terminated by arbitrary impedances," in *IEEE MTT-S Int. Microwave Symp. Dig.*, June 2000, pp. 1137–1140.
[11] G. Hanington, P.-F. Chen, P. M. Asbeck, and L. E. Larson, "High-efficiency power amplifier using dynamic power-supply voltage for CDMA applications," *IEEE Trans. Microwave Theory Tech.*, vol. 47, pp. 1471–1476, Aug. 1999.

Masaya Iwamoto (S'99) received the B.S. degree in electrical engineering from Cornell University, Ithaca, NY, in 1997, the M.S. degree in electrical engineering from the University of California at San Diego (UCSD), in 1999, and is currently working toward the Ph.D. degree at UCSD. His Ph.D. dissertation concerns the distortion characteristics of InGaP/GaAs HBTs and their applications to power amplifiers.

During the summers of 1997–2001, he was an Intern at Agilent Technologies (formerly Hewlett-Packard), Santa Rosa, CA, where he was responsible for HBT large-signal modeling, distortion characterization, and broad-band power-amplifier design.

Aracely Williams received the B.S. and M.S. degrees from the University of California at San Diego (UCSD), in 1999 and 2001, both in electrical engineering.

She is currently with the CDMA Technologies Semiconductor Division, Qualcomm, San Diego, CA. Her research interests include RF power-amplifier and RF system and circuit designs.

Pin-Fan Chen (S'92–M'99) received the B.S.E.E. degree from the University of California at Los Angeles (UCLA), in 1992, and the M.S. and Ph.D. degrees in electrical engineering from the University of California at San Diego (UCSD), in 1993 and 2001, respectively.

From 1993 to 1998, he was a Research Assistant at UCSD, where he was involved with compound semiconductor devices and circuit-related topics. These topics include resonant tunneling diode circuits, high-speed HBT logic, HBT design and fabrication, double heterojunction bipolar transistor (DHBT), and power amplifiers. In December 1998, he joined Global Communication Semiconductors Inc., Torrance, CA, where he was involved with the extraction of HBT and pseudomorphic high electron-mobility transistor (pHEMT) models as well as having established GaAs foundry flow as the Manager of the Modeling Group. In March 2001, he joined Agilent Technologies, Santa Clara, CA, where he is currently involved with GaAs enhanced–mode pHEMT (E-pHEMT) circuit developments.

Andre G. Metzger (S'93) received the B.S. and M.S. degrees in electrical engineering from the University of California at San Diego (UCSD), in 1995 and 1996, respectively, and is currently working toward the Ph.D. degree at UCSD. His doctoral dissertation concerns data recovery in dispersed fiber transmission systems.

Since 1995, he has been involved in research with the High Speed Device Group, UCSD. From 1995 to 1997, he was a key member in the design of a 12 $\times$ 12 10 Gb/s crosspoint switch that made up the core of a Defense Advanced Research Projects Agency (DARPA)-sponsored 40 Gb/s 3 $\times$ 3 opto-electronic switch project entitled WEST. He has interned with Rockwell Science Center and Conexant Systems. He is currently with Mindspeed Technologies, Newbury Park, CA, where he is involved with communications circuits for OC-192 and OC-768. His research interests include mixed-signal bipolar and CMOS circuit design, switching and millimeter-wave power-amplifier design, and HBT device design.

Lawrence E. Larson (S'82–M'82–SM'90–F'00) received the B.S. degree in electrical engineering and the M.Eng. degree from Cornell University, Ithaca, NY, in 1979 and 1980, respectively, and the Ph.D. degree in electrical engineering from the University of California at Los Angeles, in 1986.

In 1980, he joined the Hughes Research Laboratories, Malibu, CA, where he directed work on high-frequency InP, GaAs, and silicon integrated-circuit development for a variety of radar and communications applications, as well as microlectromechanical system (MEMS)-based circuits for RF and microwave applications. He was also the Assistant Program Manager of the Hughes/Defense Advanced Research Projects Agency (DARPA) Monolithic-Microwave Integrated-Circuit (MIMIC) Program from 1992 to 1994. From 1994 to 1996, he was with Hughes Network Systems, Germantown, MD, where he directed the development of RF integrated circuits for wireless communications applications. In 1996, he joined the faculty of the University of California at San Diego (UCSD), where he is the Inaugural Holder of the Communications Industry Chair. He holds 21 U.S. patents.

Dr. Larson is a member of Sigma Xi and Eta Kappa Nu. He was corecipient of the 1996 Lawrence A. Hyland Patent Award of Hughes Electronics for his work on low-noise millimeter-wave high electron-mobility transistors (HEMTs).

Peter M. Asbeck (M'75–SM'97–F'00) received the B.S. and Ph.D. degrees in electrical engineering from the Massachusetts Institute of Technology (MIT), Cambridge, in 1969 and in 1975, respectively.

He was with the Sarnoff Research Center, Princeton, NJ, and at the Philips Laboratory, Briarcliff Manor, NY, where he was involved in the areas of quantum electronics and GaAlAs/GaAs laser physics and applications. In 1978, he joined the Rockwell International Science Center, where he was involved in the development of high-speed devices and circuits using III–V compounds and heterojunctions. He pioneered the effort to develop HBTs based on GaAlAs/GaAs and InAlAs/InGaAs materials, and has contributed widely in the areas of physics, fabrication, and applications of these devices. In 1991, he joined the University of California at San Diego (UCSD), as Professor in the Department of Electrical and Computer Engineering. His research interests are in development of high-speed heterojunction transistors and opto-electronic devices, and their circuit applications.

Dr. Asbeck is a distinguished lecturer of the IEEE Electron Device Society and of the IEEE Microwave Theory and Techniques Society (IEEE MTT-S). He is a member of the Department of Defense Advisory Group on Electron Devices. He was the general chairman of the 1996 Device Research Conference, and the chairman of the 1999 IEEE Topical Workshop on Power Amplifiers for Wireless Communications.